



Since January 2020 Elsevier has created a COVID-19 resource centre with free information in English and Mandarin on the novel coronavirus COVID-19. The COVID-19 resource centre is hosted on Elsevier Connect, the company's public news and information website.

Elsevier hereby grants permission to make all its COVID-19-related research that is available on the COVID-19 resource centre - including this research content - immediately available in PubMed Central and other publicly funded repositories, such as the WHO COVID database with rights for unrestricted research re-use and analyses in any form or by any means with acknowledgement of the original source. These permissions are granted for free by Elsevier for as long as the COVID-19 resource centre remains active.



Inhibitory effect of silver nanomaterials on transmissible virus-induced host cell infections



Xiaonan Lv^{a,b,1}, Peng Wang^{b,1}, Ru Bai^b, Yingying Cong^a, Siqingowa Suo^a, Xiaofeng Ren^{a,**}, Chunying Chen^{b,*}

^a Department of Preventive Veterinary Medicine, College of Veterinary Medicine, Northeast Agricultural University, No. 59, Mucai Street, Xiangfang District, Harbin 150030, PR China

^b National Center for Nanoscience and Technology of China, No. 11, Beiyitiao, Zhongguancun, Beijing 100190, PR China

ARTICLE INFO

Article history:

Received 5 December 2013

Accepted 22 January 2014

Available online 10 February 2014

Keywords:

Silver nanomaterials

Antiviral treatment

Transmissible gastroenteritis virus

p38 MAPK signaling pathway

ABSTRACT

Coronaviruses belong to the family *Coronaviridae*, which primarily cause infection of the upper respiratory and gastrointestinal tract of hosts. Transmissible gastroenteritis virus (TGEV) is an economically significant coronavirus that can cause severe diarrhea in pigs. Silver nanomaterials (Ag NMs) have attracted great interests in recent years due to their excellent anti-microorganism properties. Herein, four representative Ag NMs including spherical Ag nanoparticles (Ag NPs, NM-300), two kinds of silver nanowires (XFJ011) and silver colloids (XFJ04) were selected to study their inhibitory effect on TGEV-induced host cell infection *in vitro*. Ag NPs were uniformly distributed, with particle sizes less than 20 nm by characterization of environmental scanning electron microscope and transmission electron microscope. Two types of silver nanowires were 60 nm and 400 nm in diameter, respectively. The average diameter of the silver colloids was approximately 10 nm. TGEV infection induced the occurring of apoptosis in swine testicle (ST) cells, down-regulated the expression of Bcl-2, up-regulated the expression of Bax, altered mitochondrial membrane potential, activated p38 MAPK signal pathway, and increased expression of p53 as evidenced by immunofluorescence assays, real-time PCR, flow cytometry and Western blot. Under non-toxic concentrations, Ag NPs and silver nanowires significantly diminished the infectivity of TGEV in ST cells. Moreover, further results showed that Ag NPs and silver nanowires decreased the number of apoptotic cells induced by TGEV through regulating p38/mitochondria-caspase-3 signaling pathway. Our data indicate that Ag NMs are effective in prevention of TGEV-mediated cell infection as a virucidal agent or as an inhibitor of viral entry and the present findings may provide new insights into antiviral therapy of coronaviruses.

© 2014 Elsevier Ltd. All rights reserved.

1. Introduction

Metal nanomaterials have received considerable attention due to their attractive physicochemical properties. In the biomedical fields, many applications for metal nanomaterials have been explored including biosensors [1], labels for cells and biomolecules [2], and cancer diagnostics and therapeutics [3]. Although the antibacterial, antifungal and antiviral properties of silver ions and silver compounds have been extensively studied and used for centuries, silver nanoparticles have shown much more superior efficacy for their promising antimicrobial potential [4], which have

been used for wound healing against bacteria [5]. Moreover, *in vitro* studies have demonstrated that spherical Ag nanoparticles (Ag NPs) can be used as antiviral agents against the human immunodeficiency virus (HIV) [6], respiratory syncytial virus [7], H1N1 influenza A virus [8], monkeypox virus [9] or hepatitis B virus [10]. However, the antiviral effects of silver nanomaterials (Ag NMs) against coronaviruses (CoVs) remain an undeveloped area.

CoVs have been very common throughout the world, as both human and animals are susceptible to them (<http://www.cdc.gov/coronavirus/>). Particularly some coronaviruses, such as severe acute respiratory syndrome coronavirus (SARS-CoV) and the recently identified Middle East respiratory syndrome coronavirus (MERS-CoV) may cause fatal infection in human. Transmissible gastroenteritis virus (TGEV), a porcine coronavirus, causes very high mortality in piglets and thus has tremendous impact of pig industry [11,12]. Vaccination has been extensively applied to prevent pigs from TGEV infection. Virulent or attenuated vaccines can

* Corresponding author. Tel.: +86 10 82545560; fax: +86 10 62656765.

** Corresponding author. Tel.: +86 45 155191974; fax: +86 45 155103336.

E-mail addresses: renxf@neau.edu.cn (X. Ren), chenchy@nanocr.cn (C. Chen).

¹ These authors contributed equally to this work.

be used to vaccinate sows and the resulting colostrum may provide protection to sucking piglets, however, the immune efficacy was not ideal and the potential dissemination as well as prevalence of infectious agent in piglets remain [13,14]. Therefore, development of preventive and therapeutic strategies is indispensable for control of TGEV infection. To date, the understanding and knowledge regarding effectiveness evaluation of chemical reagents on TGEV infection are limited. Although Ag NMs have been displaying appealing effect on antiviral research [15,16], their potential inhibitory effect on TGEV infection has not been studied and reported until now. Moreover, TGEV, like many other viruses, exerts much of its cell effect through the induction of apoptosis of its host cell [17–19]. Previous reports showed that the activation of caspases played a critical role in cell apoptosis triggered by TGEV [19–21]. However, whether and how TGEV-mediated apoptosis could be regulated by Ag NMs is unknown.

Therefore, in this study, we used TGEV as a model of CoVs and comparatively evaluated the inhibitory effect of four different Ag NMs (Ag NPs, silver nanowires 60 nm, silver nanowires 400 nm, and silver colloids) on TGEV-mediated cell infection and apoptosis. The underlying molecular mechanism was further explored. Mitochondrial membrane potential (MMP), p38 MAPK signal pathway activation, the expression of Bcl-2 family proteins and the cleavage of the precursor caspase-3 were measured.

2. Materials and methods

2.1. Preparation and characterization of Ag NMs

Four Ag NMs consisting of Ag NPs (NM-300), two kinds of silver nanowires (XFJ011) and silver colloids (XFJ04) were selected in this study. Ag NPs was supplied by the Institute for Health and Consumer Protection (IHCP, one Joint Research Centre of European Commission located in Italia) under coordination within the Project of European Commission 7th Framework Program. The others were purchased from Nanjing XFANO Materials Tech Co., Ltd., (Nanjing, China). Their size and morphology were characterized by environmental scanning electronic microscopy, ESEM (Quanta 200 FEG) or transmission electron microscopy, TEM (Tecnai G2 20 S-TWIN). The particle size distribution of Ag NPs and silver colloids was further characterized by nanoparticle tracking analysis (NanoSight LM10-Base, Nano Sight Ltd., UK). All Ag NMs were dispersed in deionized water to 1 mg/mL and were then further diluted into fresh medium to the final concentrations as required.

2.2. Cell culture and virus

Swine testicle (ST) cells were cultured in Dulbecco's modified Eagle's medium (DMEM, Gibco) supplemented with 10% fetal bovine serum (FBS, Gibco) at 37 °C with 5% CO₂. TGEV strain PUR46-MAD was propagated in ST Cells as previously described [11,13].

2.3. Cell viability assays

Toxic effects of the Ag NMs on ST cells were determined using the Mosmann-based 3-(4,5-Dimethylthiazol-2-yl)-2,5-diphenyltetrazolium bromide (MTT) assay [22]. Briefly, approximately 6×10^3 cells were plated onto 96-well plates (Corning, USA). After the cells became confluence, the cells were incubation with different concentrations of Ag NMs for 48 h at 37 °C. Then, MTT reagent was added to the cells according to the manufacturer protocol and the absorbance at 570 nm was recorded by an Infinite M200 microplate reader (Tecan, Durham, USA). Mock-treated cells served as control. Each experiment was performed in triplicate.

2.4. Antiviral activity of Ag NMs

The inhibitory effect of the Ag NMs on TGEV was determined using the MTT assay, as described previously [23–25]. Briefly, TGEV at an MOI (multiplicity of infection) of 0.5 was incubated with serially diluted Ag NMs in medium at 37 °C for 1 h. Then, ST cells cultured on 96-well plates were infected with viruses containing or not containing Ag NMs for another hour. Then the cells were washed three times with phosphate-buffered saline (PBS) and maintained in DMEM (200 μ L/well). At 48 h post-infection (hpi), the cells were incubated with MTT reagent. OD₅₇₀ values of the cells were determined as above. Sole virus-infected and mock-treated cells served as infection and blank controls, respectively. Relative amount of survival cells (%) was calculated as follows: Percentage of viable cells = $\frac{\{\text{OD of drug treatment group} - \text{OD of infection control}\}}{\{\text{OD of blank control} - \text{OD of infection control}\}} \times 100\%$.

2.5. Real-time quantitative PCR

TGEVs at an MOI of 0.5 were incubated with the indicated dose of Ag NMs (From 3.125 μ g/mL to 12.5 μ g/mL) for 1 h. Then the viruses were used to infect ST cells grown in 6-well plates as above. At 48 hpi, the total RNA was extracted using TRIzol agent (Invitrogen, Carlsbad, CA, US), and 2 μ g of each RNA sample was subjected to reverse transcription according to the manufacturer's instructions. The resulting cDNA samples were analyzed by quantitative real-time PCR (qRT-PCR) (Eppendorf, Germany) using SYBR green as fluorescence dye, as described previously [13,26]. Relative quantifications of mRNA expression of the genes of interest were calculated using the comparative threshold cycle number for each sample. The following genes were measured: S-X (a fragment comprising the 3' half of the S gene, the intervening sequence and the 3a gene), 3CLpro (a nonstructural gene encoding the 3CL protease of TGEV), Bax, Bcl-2 and beta-actin. The primers for qRT-PCR in this study were shown in Table S1.

2.6. Western blot

The samples were treated as above and the cells were harvested and washed with ice-cold PBS followed by treatment with ice-cold RIPA lysis buffer with 1 mM phenylmethyl sulfonyl fluoride (PMSF). Protein concentrations were measured using BCA Protein Assay Reagent (Pierce, Rockford, IL, US). Equivalent amounts of proteins were loaded and run on 8–12% sodium dodecyl sulfate–polyacrylamide gel electrophoresis (SDS–PAGE). Subsequently, proteins were transferred to polyvinylidene difluoride (PVDF) membranes (Millipore Corp, Atlanta, GA, US). The membranes were blocked with 5% non-fat dry milk at room temperature for 1 h, and then incubated with indicated primary antibodies overnight at 4 °C, followed by horseradish peroxidase (HRP)-conjugated secondary antibodies at room temperature for 1 h. Information on antibodies can be found in the supporting information section. Blots were developed using enhanced chemiluminescence, as described previously [26,27]. The tested proteins included Bax, Bcl-2, caspase-3, Phospho-p38 MAP Kinase (Pi-p38), p38 MAP Kinase (p38), p53, PARP and beta-actin.

2.7. Indirect immunofluorescence assays

Inhibitory effect of the Ag NMs on cell infection by TGEV was further evaluated by immunofluorescence. ST cells in 96-well plates were infected with TGEV at an MOI of 0.5, or TGEV pre-treated with Ag NPs, silver nanowires 60 nm, silver nanowires 400 nm or silver colloids respectively for 1 h. At 36 hpi, the cells were rinsed once with PBS and fixed in 4% formaldehyde for 15 min at room temperature, permeabilized with 0.1% Triton X-100 for 5 min at room temperature and incubated with the anti-TGEV polyclonal antibody (1:200 dilution) for 2 h and fluorescein isothiocyanate (FITC)-labeled goat anti-rabbit IgG (H+L) secondary antibody (1:200 dilution) for 1 h. Images were all collected using an IN cell analyzer 2000 (GE health). Nine image fields/well were captured at the same exposure time and at least 200 cells per image filed were measured for effective data output. Fluorescence density calculations were performed automatically by the IN cell analyzer software 3.7.1 (GE Healthcare, US) according to the manufacturer protocol.

2.8. Flow cytometry analysis

Cell apoptosis induced by TGEV was further analyzed with FITC Annexin V Apoptosis Detection kit (Becton Dickinson, Sunnyvale, CA) as previously described [13,28]. The above-mentioned cell samples were trypsinized and then centrifuged at 2000 rpm for 5 min. The cells were re-suspended with 500 μ L of binding buffer at a density of 10^6 cells/mL, after washing two times with PBS at 2000 rpm for 5 min. Then, 5 μ L of FITC-conjugated Annexin V and 5 μ L of propidium iodide (PI) were added to the suspension for another incubation at room temperature for 15 min in the dark. The samples were analyzed within 1 h post-staining.

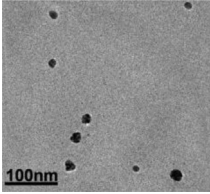
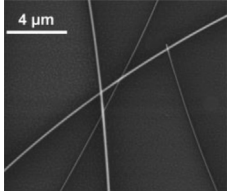
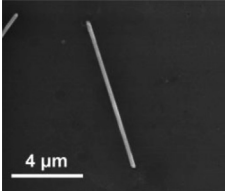
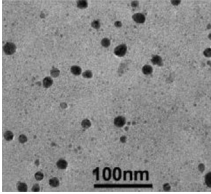
Mitochondrial membrane potential was determined using Rhodamine 123 (Invitrogen, Carlsbad, CA, US) as previously described [29]. ST cells were cultured at a density of 6×10^3 cells per well in 96-well plates in medium and incubated for 24 h. Cell samples included mock-infected ST cells or ST cells infected with TGEV at different MOIs for 12 h. Then, the cells were stained with 10 μ M of Rhodamine 123 in PBS solution with 0.4% glucose for 30 min. The cells in each dish were washed gently with PBS three times prior to Flow cytometry analysis (BD FACSCalibur™ Flow Cytometer).

3. Results and discussion

3.1. Characterization of various Ag NMs

Four types of Ag NMs were physically characterized by ESEM or TEM. As shown in Table 1, silver nanowires were 60 nm and 400 nm in diameter. Ag NPs were uniformly distributed, with particle sizes less than 20 nm. The average diameter of silver colloids was approximately 10 nm. The stabilizing agents of Ag NPs were comprised of 7% ammonium nitrate, 4% each of Polyoxyethylene

Table 1
Specifications of silver nanomaterials.

	Silver nanoparticles	Silver nanowires 60 nm	Silver nanowires 400 nm	Silver colloids
Diameter (OD)	<20 nm	60 nm	400 nm	~ 10 nm
Length		60–80 μm	20–30 μm	
Stabilizing agents	7% ammonium nitrate, 4% each of Polyoxyethylene Glycerol Trioleate and 4% Tween 20	<0.5 wt% PVP	<0.5 wt% PVP	2 wt% PVP
TEM or ESEM morphology				

Transmission electron microscopy (TEM) images of Ag NPs and silver colloids (Bar = 100 nm); environmental scanning electronic microscopy (ESEM) images of two kind of silver nanowires (Bar = 4.0 μm).

Glycerol Trioleate and 4% Tween 20. The capping agent of silver nanowires 60 nm (Ag NW60), silver nanowires 400 nm (Ag NW400) and silver colloids was PVP (Polyvinylpyrrolidone). However, the concentration of PVP used in these nanomaterials was not the same. The content of PVP in silver colloids was about four times higher than silver nanowires, which is necessary for their synthesis and their good dispersion. Silver colloids were well dispersed and had no obvious precipitation formation even at 1 mg/mL when put at room temperature for 6 months. To determine their dispersion and particle size distribution, Ag NPs and silver colloids were further characterized by nanoparticle tracking analysis (NTA), which has been reported as a powerful characterization technique that complements dynamic light scattering [30]. As shown in Fig. S1, both Ag NPs and Ag colloids were well dispersed, and their average particle size was about 30 nm. It seems that the particle size distribution data got from NTA is not consistent with the data provided by the company. Maybe it is because two or three nanoparticles bunched together during NTA. Nevertheless, the biggest size is not exceeding 100 nm, and there appeared a single peak in either Ag NPs or Ag colloids. All these findings suggest that Ag NPs and Ag colloids were well dispersed.

3.2. The cytotoxicity and anti-TGEV activity of Ag NMs in ST cells

The biological responses of nanoparticles are strongly dependent upon their physicochemical properties such as shape, size and their interactions with capping agent molecules [31–33]. To evaluate the potential cytotoxic effects of various Ag NMs on ST cells (a type of TGEV-susceptible porcine cell line), we used MTT assay to investigate the viability of ST cells incubated with different Ag NMs at a concentration ranging from 3.125 to 50 $\mu\text{g}/\text{mL}$ for 48 h. As shown in Fig. 1A, 12.5 $\mu\text{g}/\text{mL}$ Ag NPs resulted in little cytotoxicity *in vitro*. More than 80% of the cells remain unaffected by 12.5 $\mu\text{g}/\text{mL}$ Ag NPs, whereas 25 and 50 $\mu\text{g}/\text{mL}$ Ag NPs were highly toxic to ST cells. In addition, high concentrations (i.e. 50 $\mu\text{g}/\text{mL}$) of silver nanowires (60 nm, 400 nm) induced much less cell death than Ag NPs in ST cells. This might be due to the bigger size of silver nanowires than Ag NPs, and thus little silver nanowires could be taken up by ST cells. However, given the high aspect ratio of silver nanowires, the limited toxicity caused by silver nanowires may be attributed to the insertion of silver nanowires into ST cells. More interestingly, although silver colloids, which were well coated and dispersed by PVP, had a similar shape and size with Ag NPs, they caused no cytotoxicity in ST cells even at the highest dose tested

(50 $\mu\text{g}/\text{mL}$). It is well known that the surface chemistry of the nanoparticles can modify their interactions with external systems. The fact that the Ag NPs present higher cytotoxicity than PVP-coated Ag colloids can be explained in terms of surface chemistry. Since Ag NPs possess lower surface coating, they may be able to interact stronger with ST cells or easier to be taken up by ST cells, in turn increasing their toxicity.

Several studies have demonstrated that Ag NPs are promising antiviral materials [6–10]. To analyze the anti-TGEV activity of Ag NMs, ST cells were treated with a mixture combined with TGEV and Ag NMs at a concentration of 3.125–12.5 $\mu\text{g}/\text{mL}$. The S-X gene and 3CLpro gene of TGEV were used as target genes and qRT-PCR was employed to examine their expression level. As shown in Fig. 1B and C, the gene levels of S-X and 3CLpro were significantly decreased by Ag NPs, Ag NW60 and Ag NW400 in a dose-dependent manner. Nevertheless, silver colloids treatment did not cause a statistically significant change of the amplification of the two genes. These data indicate that Ag NPs and Ag nanowires possess significant anti-TGEV activity, but silver colloids have no effect on TGEV multiplication. The low anti-TGEV activity of PVP-coated silver colloids can also be explained in terms of surface chemistry. Although silver nanowires are also coated with PVP, however, on one hand, the PVP concentration used in silver nanowires is lower than in silver colloids; on the other hand, silver nanowires may be more difficult to be well coated and dispersed by PVP due to their high-aspect-ratio. Thus, the coated PVP may participate in reducing the free Ag surfaces exposed directly to cells and virus, which is responsible for Ag NMs-mediated cytotoxicity and antiviral activity.

To further confirm the inhibitory effects of Ag NPs and silver nanowires on TGEV multiplication, immunofluorescence was performed to examine the amount of TGEV in ST cells. As shown in Fig. 1D and E, both Ag NPs and two types of nanowires could significantly decrease the number of TGEV-infected cells. The results indicate that Ag NPs and Ag nanowires, which have thinner PVP-coating than Ag colloids, could be easier to interact with ST cell membranes or TGEV surface proteins to inhibit TGEV infection and multiplication.

3.3. The inhibitory effect of Ag NMs on TGEV-induced cell apoptosis

TGEV infection is generally acute and causes a high mortality rates (up to 100%) in seronegative suckling piglets [34]. Our previous work and other reports have proved that TGEV infection may

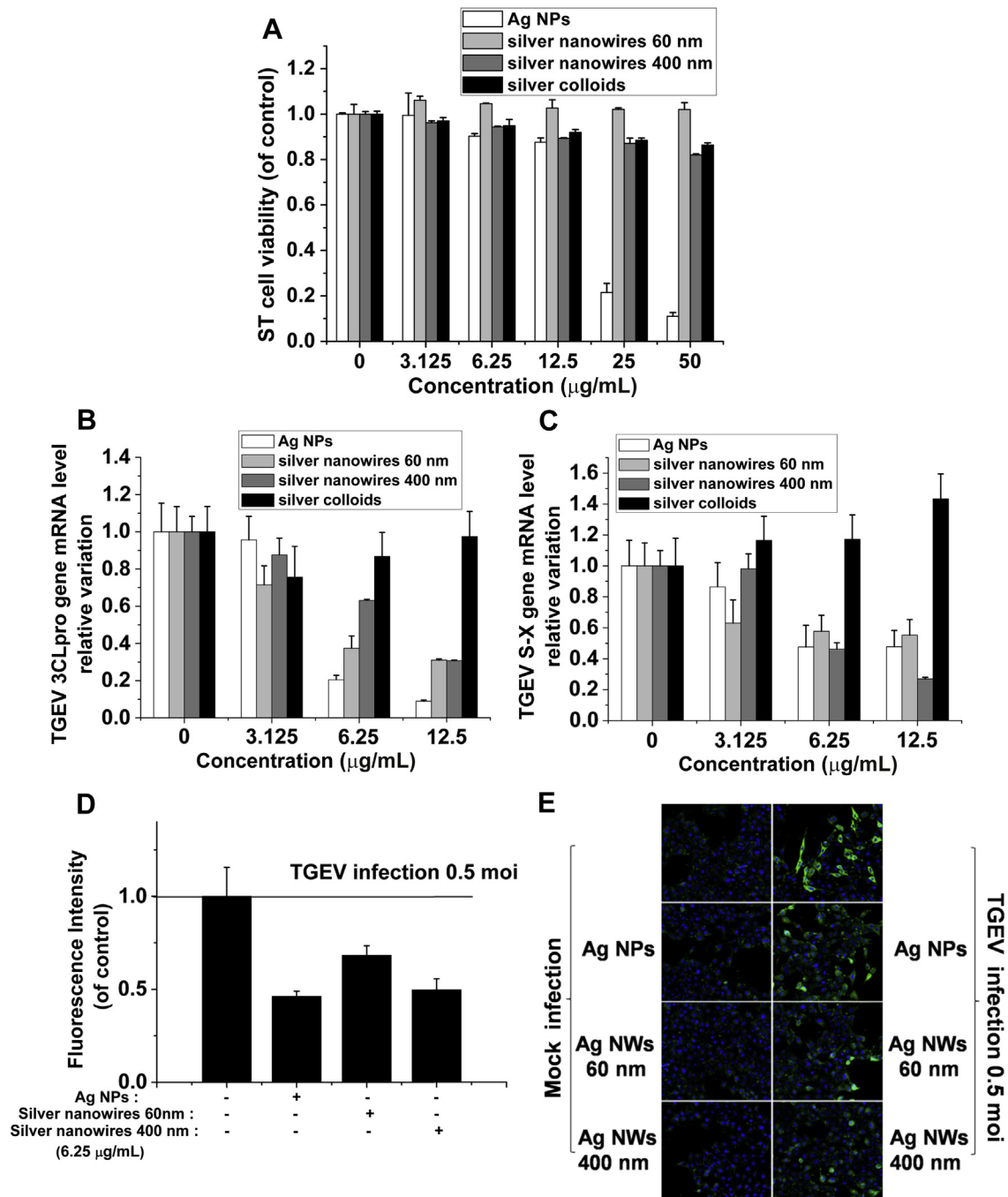


Fig. 1. The cytotoxicity and anti-TGEV activity of Ag NMs in ST cells. (A) ST cells were pretreated with the indicated doses of Ag NMs for 1 h, and then washed three times with PBS and cultured in DMEM for another 48 h. Cell viability was measured by MTT. All the MTT values were normalized to the control (no Ag NMs exposure), which represents 100% cell viability. (B, C) TGEV was first incubated with various Ag NMs *in vitro* for 1 h. Next, ST cells were infected by TGEV combined with the indicated doses of Ag NMs for 1 h, and then washed three times with PBS and cultured in DMEM for another 48 h. RNA was extracted and real time quantitative PCR was performed using 2 μg of total RNA for S-X (B) and 3CLpro (C). (D, E) The protein expression of TGEV S was analyzed by immunofluorescence at 36 hpi. Representative fluorescence images of TGEV S (green) and nuclei (blue) were acquired (D) and counted (E) by the IN Cell HCS system. All results are expressed as mean ± SD of at least three independent experiments. (For interpretation of the references to colour in this figure legend, the reader is referred to the web version of this article.)

be associated with host cell apoptosis [13,19–21], which may be the reason for TGEV-induced fatal diarrhea in newborn pigs. In the present work, we firstly observed the morphological changes of TGEV-infected ST cells. As shown in Fig. 2A, the cytopathic effect of ST cells was typical at 36 hpi and became more evident at 48 hpi, compared to the mock-infected cells. This result indicated that TGEV infection caused cell death in ST cells. To further confirm the effect of Ag NMs on TGEV induced host cell apoptosis, TGEV-

infected ST cells were analyzed by Annexin V-FITC and PI dual staining kit. Early apoptotic cells could be stained with Annexin V but not PI. Fig. 2B showed that at 24 hpi, the early apoptotic rate of cells infected by the virus control was 10.07%, however, in cells treated with the combined mixture of virus and Ag NMs, the apoptotic rate was downregulated to 5.33% (Ag NPs), 4.97% (Ag NW60) and 4.93% (Ag NW400), respectively, which indicated that Ag NMs had an inhibitory activity against TGEV-induced cell

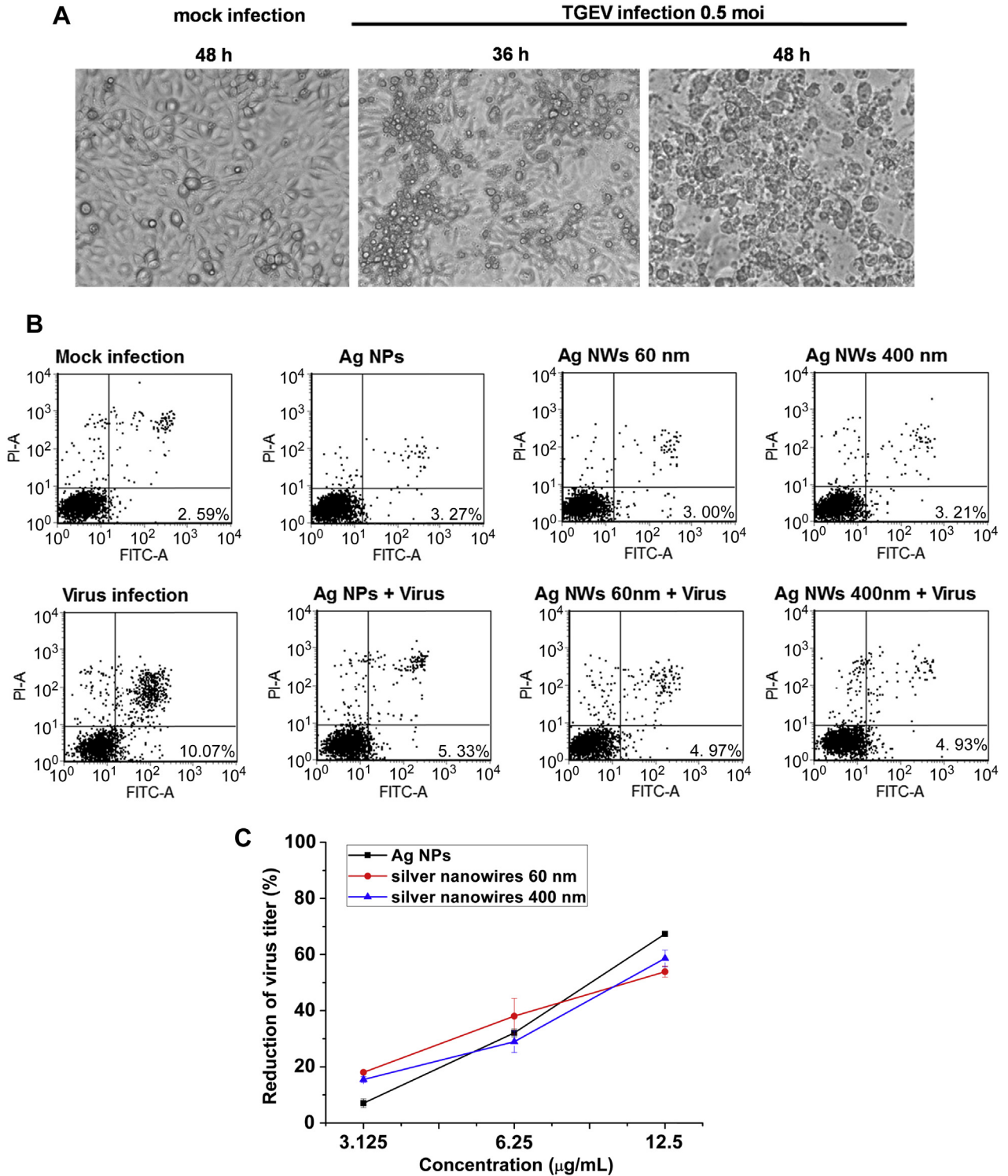


Fig. 2. The inhibitory effect of Ag NMs on TGEV-induced cell apoptosis. (A) Cells were seeded into 24-well culture plates and infected with TGEV (MOI 0.5) for different time points. The morphological changes in TGEV-infected cells were observed by optical microscope. (B) ST cells were infected by TGEV or TGEV combined with 6.25 $\mu\text{g/mL}$ Ag NMs for 1 h, and then the cells were collected at 24 hpi and stained with Annexin V-FITC and PI. Cell apoptosis was analyzed by flow cytometry. The early apoptosis rates of cells are indicated. (C) TGEV (MOI 0.5) were incubated with indicated doses of Ag NMs at 37 $^{\circ}\text{C}$ for 1 h in DMEM. Then the pretreated complexes were used to infect cells at 37 $^{\circ}\text{C}$ for 1 h in 96-well plates. Cell viability was measured by MTT at 48 hpi. The results are expressed as mean \pm SD of at least three independent experiments.

apoptosis. Moreover, we further employed MTT assay to examine the effect of Ag NMs on TGEV-induced cell viability inhibition. Compared with the virus control (without treatment of Ag NMs), Ag NMs (Ag NPs, silver nanowires 60 nm and 400 nm) which were at a concentration of 3.125–12.5 $\mu\text{g/mL}$ exhibited a dose-dependent

anti-TGEV activity at 48 hpi (Fig. 2C). The percentage reduction in virus titer caused by Ag NMs at a concentration of 3.125 $\mu\text{g/mL}$ was 7.05 \pm 1.57% (Ag NPs), 18.04 \pm 0.66% (Ag NW60) and 15.48 \pm 1.00% (Ag NW400). At 6.25 $\mu\text{g/mL}$, the percentage reduction was 32.12 \pm 1.43% (Ag NPs), 38.06 \pm 6.31% (Ag NW60) and

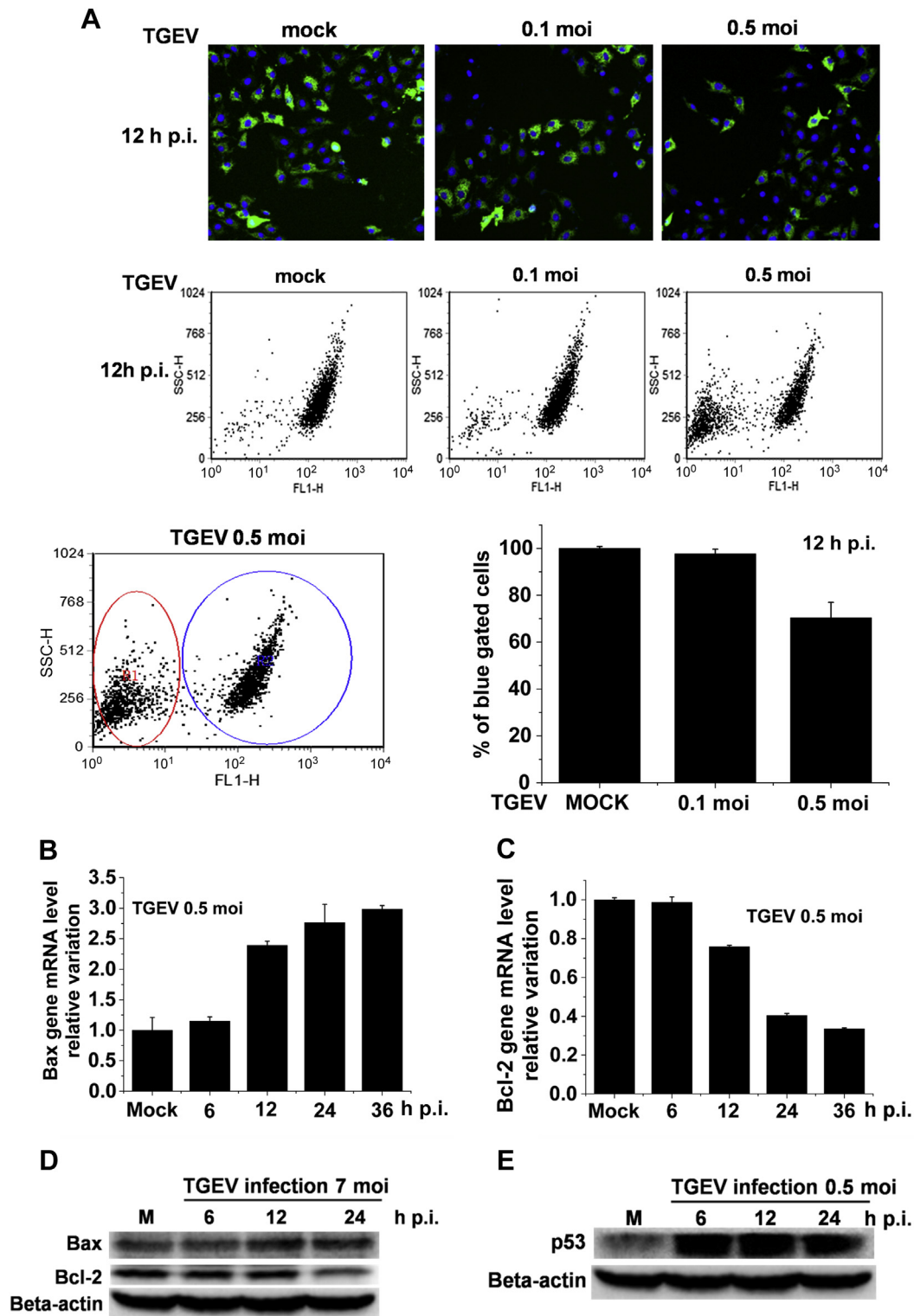


Fig. 3. TGEV infection induced cell apoptosis by regulating mitochondrial membrane potential (MMP) and the expression of Bcl-2 family proteins. (A) ST Cells were mock-infected or TGEV-infected at different MOIs for 12 h and stained with Rhodamine 123 (green) and Hoechst 33342 (blue). Representative fluorescence images were acquired by fluorescence microscopy. MMP was analyzed by flow cytometry. (B, C) ST Cells were mock-infected or TGEV-infected (MOI 0.5) for different times, and then prepared for RNA isolation. Real time quantitative PCR was performed using 2 μ g of total RNA for Bcl-2 (B) and Bax (C). (D) Western blot analysis of the expression of the Bcl-2 and Bax in ST cells infected by TGEV with different times. (E) The accumulation of p53 in TGEV-infected ST cells were analyzed by Western blot. The results are expressed as mean \pm SD of at least three independent experiments. (For interpretation of the references to colour in this figure legend, the reader is referred to the web version of this article.)

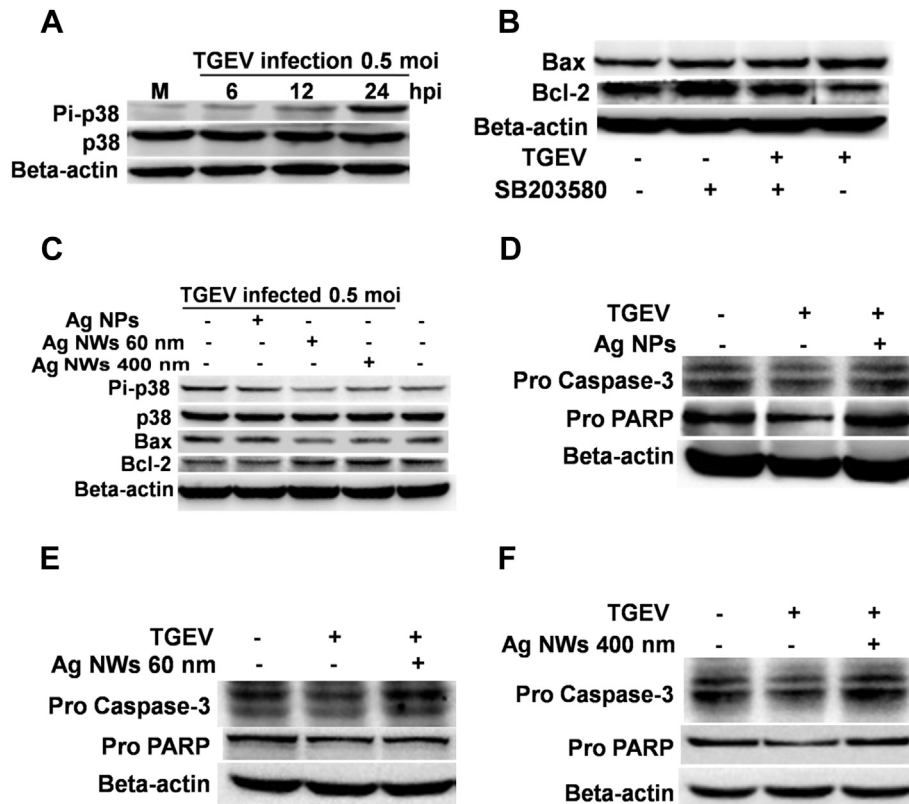


Fig. 4. Ag NMs inhibit cell apoptosis during TGEV infection via regulating p38/mitochondria-caspase-3-mediated apoptotic pathway. (A) ST cells were mock-infected or TGEV-infected (MOI 0.5) for different times and then the cell lysates were analyzed by Western blot. (B) ST cells were exposed to TGEV with or without addition of SB203580, a specific inhibitor of p38 MAPK, and then the protein level of Bcl-2 and Bax was determined by Western blot. (C) ST cells were infected by TGEV or TGEV combined with 6.25 $\mu\text{g}/\text{mL}$ Ag NMs for 1 h, and then the cells were collected at 24 hpi. Western blot analysis was performed to examine the expression of Pi-p38, p38, Bax and Bcl-2. (D–F) ST cells were infected by TGEV or TGEV combined with 6.25 $\mu\text{g}/\text{mL}$ Ag NMs for 1 h, and then the cells were collected at 48 hpi. The protein level of Pro caspase-3 and Pro PARP were determined by Western blot. (For interpretation of the references to colour in this figure legend, the reader is referred to the web version of this article.)

$28.94 \pm 3.84\%$ (Ag NW400). At 12.5 $\mu\text{g}/\text{mL}$, the percentage reduction was $67.35 \pm 0.68\%$ (Ag NPs), $53.90 \pm 1.95\%$ (Ag NW60) and $58.65 \pm 2.95\%$ (Ag NW400). All these results suggest that Ag NMs (Ag NPs, silver nanowires 60 nm and 400 nm) not only own anti-TGEV activities but also inhibit cell apoptosis induced by TGEV infection.

3.4. The mechanism of TGEV-caused cell apoptosis

Depolarization of mitochondrial membrane potential (MMP) has been shown to participate in the induction of apoptosis [35]. To explore the mechanism of TGEV-induced apoptosis in ST cells, we first investigated whether MMP changes were induced in TGEV-infected ST cells. Compared with the untreated ST cells (control), the MMP in TGEV-infected ST cells was notably depolarized in a dose-dependent manner (Fig. 3A), implying the destruction of mitochondria integrity in TGEV-infected ST cells. Moreover, Bcl-2/Bax ratio is considered as a predictive marker in mitochondria-mediated apoptotic pathway [18,21,36]. The pro-apoptotic protein Bax induce the permeabilization of mitochondrial membrane, allowing proteins in the mitochondrial intermembrane space, such as cytochrome C, to escape into the cytosol where they can induce caspase activation and cell apoptosis [37]. Bcl-2, the major anti-apoptotic protein, can inhibit Bax-mediated mitochondrial membrane permeabilization [38]. Therefore, we subsequently examined the mRNA levels and protein levels of Bcl-2 and Bax in TGEV-infected ST cells by qRT-PCR and Western blot. The results showed that the mRNA level of Bcl-2 significantly diminished at

12 hpi, and continuously increased until 36 hpi (Fig. 3B). The mRNA level of Bax was significantly increased in TGEV-infected cells at 12 hpi and continued to increase over infection time (Fig. 3C). In accordance with the changes at the transcriptional level, the protein level of Bax was also up-regulated in a time-dependent manner in TGEV-infected cells; while the protein level of Bcl-2 was down-regulated in a time-dependent manner (Fig. 3D). These results suggest that up-regulation of Bax and decrease of Bcl-2 induced by TGEV infection may play important roles in TGEV-mediated apoptosis in ST cells.

In addition, the tumor suppressor protein p53, a major transcription factor for the control of apoptosis, has been considered to be responsible for both the decrease in the expression of the apoptosis-suppressing gene Bcl-2 and the increase in the expression of Bax [39]. Therefore, we further examined the association of TGEV infection with the expression of p53 by Western blot. The data show that the expression of p53 in TGEV-infected ST cells was up-regulated in a time-dependent manner (Fig. 3E).

The above findings decipher the relationship between TGEV infection and mitochondria-mediated apoptotic pathway. Next, we further explored the possible mechanisms by which Ag NMs inhibit cell apoptosis induced by TGEV infection.

3.5. Inhibition of TGEV-induced apoptotic signaling cascades by Ag NMs

Activation of p38 and p53 has been suggested to play important roles in TGEV-induced host cell apoptosis [40]. To further investigate

whether TGEV induced ST cell apoptosis through activation of p38 MAPK-p53-mitochondria signaling cascades, we assessed the kinetics of p38 MAPK phosphorylation by Western blot. As shown in Fig. 4A, the expression level of phosphorylated p38 (Pi-p38) was increased in a time-dependent manner and appeared the most significant increase at 24 hpi in TGEV-infected ST cells. Next we further examined whether TGEV-stimulated p38 phosphorylation could participate in the regulation of Bcl-2 and Bax expression. SB203580, a specific inhibitor of p38-MAPKs [41] was used to inhibit TGEV-induced p38 phosphorylation, and then the expression of Bcl-2 and Bax was analyzed by Western blot. In the presence of 25 μM SB203580, the activation of p38 was significantly blocked in TGEV-infected cells (data not shown). Moreover, SB203580 treatment could significantly inhibit TGEV-induced Bax expression, and restore the expression of Bcl-2, which was down-regulated by TGEV infection (Fig. 4B). These findings indicate that TGEV-induced increase of Bcl-2/Bax ratio, which plays important roles in mitochondrial-mediated apoptosis, is dependent on TGEV-mediated activation of p38 MAPK.

As mentioned above, our data demonstrated that TGEV could activate p38 MAPK, cause p53 accumulation, regulate the expression of Bcl-2 family proteins, induce the depolarization of mitochondria, and finally mediate the apoptosis of ST cells. We also found that Ag NMs caused an inhibitory effect on TGEV-induced apoptosis. To determine whether Ag NMs could inhibit TGEV-induced apoptosis through regulating p38 MAPK-p53-mitochondria signaling cascades, we next employed Western blot to quantify the expression of Pi-p38, Bcl-2 and Bax in ST cells exposed to mixtures combined with TGEV and Ag NMs. As shown in Fig. 4C, Ag NMs treatment could significantly inhibit TGEV-induced expression of Pi-p38 and Bax, but increase the expression of Bcl-2 protein. These data were in accord with the inhibitory effect of Ag NMs on TGEV-induced apoptosis and suggested that p38 MAPK-p53-mitochondria signaling cascades might be critical for Ag NMs-caused inhibitory effect on TGEV-induced apoptosis.

Furthermore, it has been documented that apoptosis is related to the activation and cleavage of the precursor caspase-3, which plays a critical role in maintaining the apoptotic signal induced by various stimulus [21,26]. Importantly, caspases-3 has been considered as a critical mediator of mitochondrial events of apoptosis [42]. Therefore, in this study, we next tried to figure out whether the anti-apoptotic effect of Ag NMs could be explained by an inhibition of caspase-3 activation. As shown in Fig. 4D, E and 4F, the level of precursor caspase-3 (pro caspase-3) was reduced in TGEV-infected cells, but drastically recovered in cells treated with TGEV plus Ag NMs. We also examined the caspase-3-mediated cleavage of precursor PARP (pro PARP) by Western blot. The results showed that caspase-3-mediated cleavage of precursor PARP in cells treated with TGEV plus Ag NMs was much less than in the cells only infected with TGEV (Fig. 4D, E and 4F). All these results indicate that Ag NMs inhibit apoptosis during TGEV infection via regulating p38/mitochondria-caspase-3-mediated apoptotic pathway.

As shown in Fig. 5, the present data suggest a possible mechanism involved in Ag NM-caused TGEV inhibition. Ag NMs including Ag NPs and silver nanowires may directly interact with TGEV surface protein, such as TGEV S glycoprotein, thus inhibit the initiation of TGEV infection. TGEV S glycoprotein is the dominant surface protein that responsible for inducing neutralizing antibodies and initiating infection [43–46]. Binding of the S glycoprotein to the cellular receptor porcine aminopeptidase N (pAPN) is required for the initiation of TGEV infection [47]. It is possible that Ag NPs and Ag nanowires could alter the structure of some surface proteins of TGEV and then inhibit their recognition and adhesion of the cellular receptor pAPN. However, silver colloids, which are well coated and dispersed by PVP, may cause limited effect on the activity of TGEV. Nevertheless, future studies will be focused on the underlying

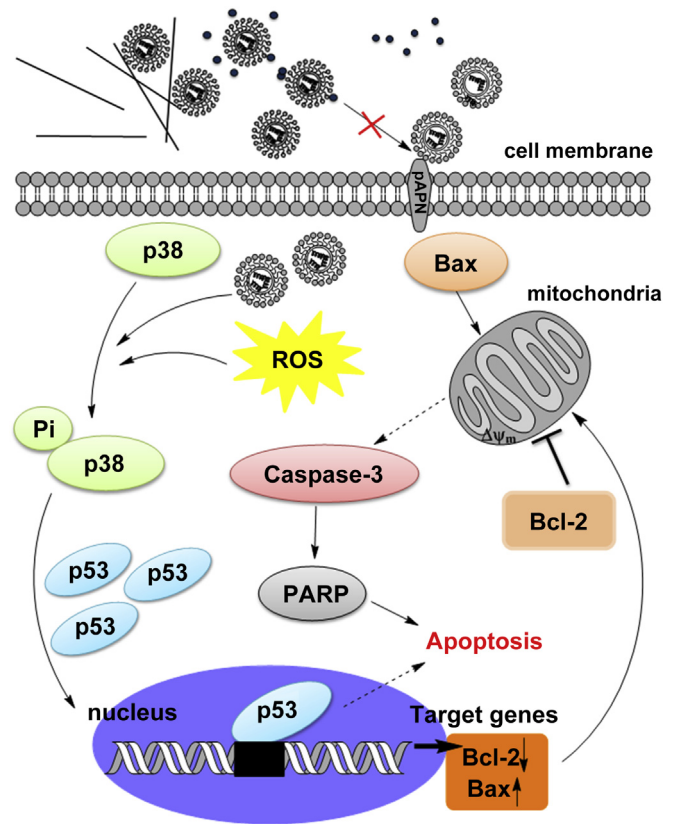


Fig. 5. Inhibitory effects of various silver nanomaterials on TGEV-induced host cell infection and p38/mitochondria-caspase-3 signaling activation. The proposed model shows that TGEV causes cell apoptosis through activation of p38 MAPK-p53-mitochondria-caspase-3 apoptotic cascades, which could be inhibited by Ag NPs and silver nanowires.

molecular mechanisms by which the effective anti-TGEV Ag NMs interact with TGEV by using experimental studies and large-scale molecular-dynamics simulations.

4. Conclusion

In the present study, four different types of Ag NMs were used to study the antiviral activity of silver against coronaviruses. Among these Ag NMs, Ag NPs and two types of silver nanowires could significantly cause an inhibitory effect on TGEV (a type of coronavirus)-induced host cell infection and TGEV multiplication. Moreover, these three Ag NMs decreased cell apoptosis which was caused by TGEV infection through activation of p38/mitochondria-caspase-3 signaling in ST cells. However, silver colloids, which are well coated and dispersed by PVP, caused no inhibitory effect on TGEV infection and multiplication. The antiviral use of metal nanomaterials had been developed by interfering with viral infection during attachment and entry. A direct interaction between the nanomaterials and the virus surface proteins could be demonstrated as the antiviral mechanism of Ag NMs. Our findings shed new light on the potential antiviral activity of Ag NMs against coronaviruses and provide new insights into the mechanisms by which Ag NMs inhibit cell apoptosis induced by TGEV infection.

Conflicts of interest statement

The authors report no conflicts of interest. The authors alone are responsible for the content and writing of the paper.

Acknowledgments

This work was financially supported by the National Basic Research Program of China (973 Program) from the Ministry of Science and Technology (2011CB933401 and 2012CB934003), the National Natural Science Foundation of China (21320102003, 31372438 and 31000337), the International Science & Technology Cooperation Program of China, Ministry of Science Technology of China (2013DFG32340 and 2014DFG52500), and sponsored by the Chang Jiang Scholar Candidates Program for Provincial Universities in Heilongjiang (2013CJHB002).

Appendix A. Supplementary data

Supplementary data related to this article can be found at <http://dx.doi.org/10.1016/j.biomaterials.2014.01.054>.

References

- Nam JM, Thaxton CS, Mirkin CA. Nanoparticle-based bio-bar codes for the ultrasensitive detection of proteins. *Science* 2003;301:1884–6.
- Zhang Z, Wang J, Chen C. Near-infrared light-mediated nanoplatforams for cancer thermo-chemotherapy and optical imaging. *Adv Mater* 2013;25:3869–80.
- Li YF, Chen C. Fate and toxicity of metallic and metal-containing nanoparticles for biomedical applications. *Small* 2011;7:2965–80.
- Sondi I, Salopek-Sondi B. Silver nanoparticles as antimicrobial agent: a case study on *E. coli* as a model for Gram-negative bacteria. *J Colloid Interface Sci* 2004;275:177–82.
- Wright J, Lam K, Hansen D, Burrell R. Efficacy of topical silver against fungal burn wound pathogens. *Am J Infect Control* 1999;27:344–50.
- Elechiguerra JL, Burt JL, Morones JR, Camacho-Bragado A, Gao X, Lara HH, et al. Interaction of silver nanoparticles with HIV-1. *J Nanobiotechnol* 2005;3:1–10.
- Sun L, Singh AK, Vig K, Pillai SR, Singh SR. Silver nanoparticles inhibit replication of respiratory syncytial virus. *J Biomed Nanotechnol* 2008;4:149–58.
- Xiang DX, Chen Q, Pang L, Zheng CL. Inhibitory effects of silver nanoparticles on H1N1 influenza A virus *in vitro*. *J Virol Methods* 2011;178:137–42.
- Rogers JV, Parkinson CV, Choi YW, Speshock JL, Hussain SM. A preliminary assessment of silver nanoparticle inhibition of monkeypox virus plaque formation. *Nanoscale Res Lett* 2008;3:129–33.
- Lu L, Sun R, Chen R, Hui CK, Ho CM, Luk JM, et al. Silver nanoparticles inhibit hepatitis B virus replication. *Antivir Ther* 2008;13:253–62.
- Ren X, Glende J, Yin J, Schwegmann-Wessels C, Herrler G. Importance of cholesterol for infection of cells by transmissible gastroenteritis virus. *Virus Res* 2008;137:220–4.
- Zhao Q, Zhu J, Zhu W, Li X, Tao Y, Lv X, et al. A monoclonal antibody against transmissible gastroenteritis virus generated via immunization of a DNA plasmid bearing TGEV S1 gene. *Monoclon Antib Immunodiagn Immunother* 2013;32:50–4.
- Ren X, Meng F, Yin J, Li G, Li X, Wang C, et al. Action mechanisms of lithium chloride on cell infection by transmissible gastroenteritis coronavirus. *PLoS One*; 2011. <http://dx.doi.org/10.1371/journal.pone.0018669>.
- Zou H, Zarlenga DS, Sestak K, Suo S, Ren X. Transmissible gastroenteritis Virus; identification of M protein-binding peptide ligands with antiviral and diagnostic potential. *Virus Res* 2013;99:383–90.
- Baram-Pinto D, Shukla S, Perkas N, Gedanken A, Sarid R. Inhibition of herpes simplex virus type 1 infection by silver nanoparticles capped with mercaptoethane sulfonate. *Bioconjug Chem* 2009;20:1497–502.
- Mehrbod P, Motamed N, Tabatabaean M, Estyar RS, Amini E, Shahidi M, et al. *In vitro* antiviral effect of “nanosilver” on influenza virus. *J Pharm Sci* 2009;17: 88–93.
- Everett H, McFadden G. Apoptosis: an innate immune response to virus infection. *Trends Microbiol* 1999;7:160–5.
- Lee SM, Kleiboeker SB. Porcine reproductive and respiratory syndrome virus induces apoptosis through a mitochondria-mediated pathway. *Virology* 2007;365:419–34.
- Eleouet JF, Chilmonczyk S, Besnardeau L, Laude H. Transmissible gastroenteritis coronavirus induces programmed cell death in infected cells through a caspase-dependent pathway. *J Virol* 1998;72:4918–24.
- Eléouët J-F, Slee EA, Saurini F, Castagné N, Poncet D, Garrido C, et al. The viral nucleocapsid protein of transmissible gastroenteritis coronavirus (TGEV) is cleaved by caspase-6 and-7 during TGEV-induced apoptosis. *J Virol* 2000;74: 3975–83.
- Ding L, Xu X, Huang Y, Li Z, Zhang K, Chen G, et al. Transmissible gastroenteritis virus infection induces apoptosis through FasL- and mitochondria-mediated pathways. *Vet Microbiol* 2012;158:12–22.
- Denizot F, Lang R. Rapid colorimetric assay for cell growth and survival: modifications to the tetrazolium dye procedure giving improved sensitivity and reliability. *J Immunol Methods* 1986;89:271–7.
- Sui X, Yin J, Ren X. Antiviral effect of diammonium glycyrrhizinate and lithium chloride on cell infection by pseudorabies herpesvirus. *Antivir Res* 2010;85: 346–53.
- Baba C, Yanagida K, Kanzaki T, Baba M. Colorimetric lactate dehydrogenase (LDH) assay for evaluation of antiviral activity against bovine viral diarrhoea virus (BVDV) *in vitro*. *Antivir Chem Chemother* 2005;16:33–9.
- Müller V, Chávez JH, Reginatto FH, Zucolotto SM, Niero R, Navarro D, et al. Evaluation of antiviral activity of South American plant extracts against herpes simplex virus type 1 and rabies virus. *Phytother Res* 2007;21:970–4.
- Li Y, Liu Y, Fu Y, Wei T, Le Guyader L, Gao G, et al. The triggering of apoptosis in macrophages by pristine graphene through the MAPK and TGF- β signaling pathways. *Biomaterials* 2012;33:402–11.
- Liu Y, Li W, Lao F, Liu Y, Wang L, Bai R, et al. Intracellular dynamics of cationic and anionic polystyrene nanoparticles without direct interaction with mitotic spindle and chromosomes. *Biomaterials* 2011;32:8291–303.
- van Engeland M, Ramaekers X, Schutte B, Reutelingsperger CP. A novel assay to measure loss of plasma membrane asymmetry during apoptosis of adherent cells in culture. *Cytometry* 1996;24:131–9.
- Lee WK, Spielmann M, Bork U, Thévenod F. Cd $^{2+}$ -induced swelling-contraction dynamics in isolated kidney cortex mitochondria: role of Ca $^{2+}$ uniporter, K $^{+}$ cycling, and protonmotive force. *Am J Physiol Cell Physiol* 2005;289:C656–64.
- Filipe V, Hawe A, Jiskoot W. Critical evaluation of nanoparticle tracking analysis (NTA) by nanosight for the measurement of nanoparticles and protein aggregates. *Pharm Res* 2010;27:796–810.
- Burda C, Chen X, Narayanan R, El-Sayed MA. Chemistry and properties of nanocrystals of different shapes. *Chem Rev* 2005;105:1025–102.
- Qu Y, Li W, Zhou YL, Liu XF, Zhang LL, Wang LM, et al. Full assessment of fate and physiological behavior of quantum dots utilizing *Caenorhabditis elegans* as a model organism. *Nano Lett* 2011;11:3174–83.
- Wang P, Nie X, Wang Y, Li Y, Ge C, Zhang L, et al. Multiwall carbon nanotubes mediate macrophage activation and promote pulmonary fibrosis through TGF- β /Smad signaling pathway. *Small* 2013;9:1799–811.
- Penzes Z, González JM, Calvo E, Izeta A, Smerdou C, Méndez A, et al. Complete genome sequence of transmissible gastroenteritis coronavirus PUR46-MAD clone and evolution of the Purdue virus cluster. *Virus Genes* 2001;23:105–18.
- Jiang X, Foldbjerg R, Miclaus T, Wang L, Singh R, Hayashi Y, et al. Multiplatform genotoxicity analysis of silver nanoparticles in the model cell line CHO-K1. *Toxicol Lett* 2013;222(1):55–63.
- Vaux DL, Strasser A. The molecular biology of apoptosis. *Proc Natl Acad Sci U S A* 1996;93:2239–44.
- Green DR, Kroemer G. The pathophysiology of mitochondrial cell death. *Science* 2004;305:626–9.
- Shimizu S, Narita M, Tsujimoto Y. Bcl-2 family proteins regulate the release of apoptogenic cytochrome c by the mitochondrial channel VDAC. *Nature* 1999;399:483–7.
- Miyashita T, Krajewski S, Krajewska M, Wang HG, Lin H, Liebermann DA, et al. Tumor suppressor p53 is a regulator of bcl-2 and bax gene expression *in vitro* and *in vivo*. *Oncogene* 1994;9:1799–805.
- Huang Y, Ding L, Li Z, Dai M, Zhao X, Li W, et al. Transmissible gastroenteritis virus infection induces cell apoptosis via activation of p53 signaling. *J Gen Virol* 2013;94:1807–17.
- Clerk A, Sugden PH. The p38-MAPK inhibitor, SB203580, inhibits cardiac stress-activated protein kinases/c-Jun N-terminal kinases (SAPKs/JNKs). *FEBS Lett* 1998;426:93–6.
- Lakhani SA, Masud A, Kuida K, Porter GA, Booth CJ, Mehal WZ, et al. Caspases 3 and 7: key mediators of mitochondrial events of apoptosis. *Science* 2006;311: 847–51.
- Enjuanes L, Suñé C, Gebauer F, Smerdou C, Camacho A, Antón IM, et al. Antigen selection and presentation to protect against transmissible gastroenteritis coronavirus. *Vet Microbiol* 1992;33:249–62.
- Gebauer F, Posthumus W, Correa I, Sae C, Smerdou C, Sanchez CM, et al. Residues involved in the antigenic sites of transmissible gastroenteritis coronavirus S glycoprotein. *Virology* 1991;183:225–38.
- Schwegmann-Wessels C, Zimmer G, Schröder B, Breves G, Herrler G. Binding of transmissible gastroenteritis coronavirus to brush border membrane sialoglycoproteins. *J Virol* 2003;77:11846–8.
- Meng F, Ren Y, Suo S, Sun X, Li X, Li P, et al. Evaluation on the efficacy and immunogenicity of recombinant DNA plasmids expressing spike genes from porcine transmissible gastroenteritis virus and porcine epidemic diarrhoea virus. *PLoS One*; 2013. <http://dx.doi.org/10.1371/journal.pone.0057468>.
- Delmas B, Gelfi J, L'Haridon R, Vogel LK, Sjöström H, Norén O, et al. Aminopeptidase N is a major receptor for the enteropathogenic coronavirus TGEV. *Nature* 1992;357:417–20.